CFD MODELING OF 2D AEROFOIL DYNAMIC STALL

L.I. Garipova *, A.N. Kusyumov *, G. Barakos *
* Kazan National Research Technical University n.a. A.N.Tupolev,
** School of Engineering - The University of Liverpool

Abstract

This work aims to investigate the dynamic stall in 2D of a NACA23012 aerofoil. In-plane motion, pitching and flapping of the section were considered as idealizations of the motion of a helicopter rotor blade section. Aerodynamic predictions are obtained using a time-accurate Navier-Stokes solver coupled with the k-ω turbulence model. The results show substantial changes of all aerodynamic coefficients and demonstrate significant differences from simple steady, or unsteady aerofoil theory.

1 Introduction

One important issue of helicopter aerodynamics is trimming. The main task of helicopter trimming is to determinate values of collective and cyclic pitch angles. A simple helicopter trimming method can be based on the Blade Element Momentum Theory (BEMT). The drawback of this theory is that it is largely based on steady-state aerofoil aerodynamics. Even for straight and level flight the aerodynamics of the helicopter blade sections can be difficult to predict. Furthermore, the aerofoil characteristics under unsteady flow can be significantly different from their steady-state equivalents [1, 2, 3].

The aim of this work is to simulate the flow around aerofoils under dynamic conditions, that correspond to forward flight cases of helicopter rotors.

2 Numerical approach

This research is conducted using computational fluid dynamics (CFD). For numerical simulation the HMB code (Helicopter Multi-Block, University of Liverpool) is used. HMB is an "in house" solver that is specialized in helicopter modeling. The simulation is based on the Reynolds averaged Navier-Stokes equations for unsteady case using k-ω SST turbulence model [4]. This turbulence model was selected as wide distributed and well-established.

For CFD meshing, multi-block structured hexa-grids were used, built using the ANSYS ICEM-Hexa tool. C-type mesh topologies were used to allow high resolution of the boundary layer for aerofoil geometry. Blocks are distributed in HMB for uniform CPU load during parallel computing.

2.1 Object of Investigation

The NACA 23012 aerofoil was selected for computations. Preliminary results in [5] considered the selection of the mesh parameters. In this work, the grid with 140,000 cells is used (Fig.1).

Results of helicopter rotor trimming were used to determine the flow conditions for aerofoil. The rotor parameters are presented in Table 1.
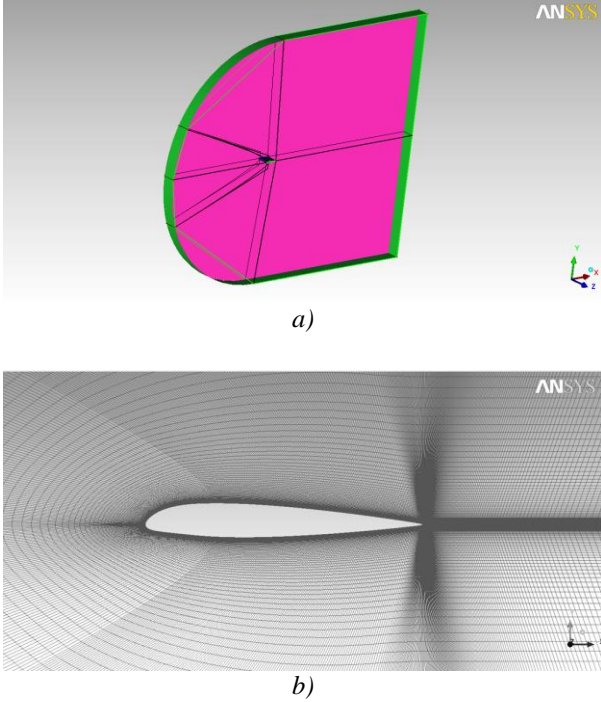
a)

b)

Fig. 1. *Topology (a) and grid (b) around the aerofoil*

Table 1. Rotor parameters

Rotor parameter	Value
Radius of rotor	5.75m
Blades number	4
Chord	0.32 m
Root radius	1.44 m
Tip velocity	220 m/s
Reynolds number	$4,86 \cdot 10^6$
Twist	5.3 deg
Shaft angle	4.5 deg

2.2 Flow conditions

Rotor trimming was conducted based on the Bramwell's algorithm [6]. Trimming was conducted for straight and level flight conditions, at an advance ratio μ of 0.15, and thrust coefficient CT of 0.01. The distribution of angle of attack is presented in Fig. 2. The angles of attack that presented at this figure were calculated taking into account non-uniform rotor downwash. Downwash induced velocity was calculated using Glauert's formula [6].

A set of radial stations were considered for modelling at r/R of 0.25, 0.35, 0.45, 0.55, 0.65, 0.75, 0.85 and 0.95. For each section the dependence of angle of attack (α) on the azimuth angle was represented as a harmonic law (1) with the number of harmonics from 1 to 5.

$$\alpha(t) = \alpha_0 + \sum_{i=1}^{5} \alpha_{ci} \cdot \cos(i \cdot \omega t) + \\ + \sum_{i=1}^{5} \alpha_{si} \cdot \sin(i \cdot \omega t) \qquad (1)$$

The free stream velocity is also unsteady, and varies according to:

$$V(t) = V_{tip} \cdot r + V_{helicopter} \cdot \sin(\omega t) \qquad (2)$$

The total velocity is represented as a superposition of a constant component, determined by the rotational frequency, and a time-variable component, determined by the velocity of the helicopter and the azimuthal position of the blade. The variable component is accounted for via mesh movement in the fore-aft directions according to:

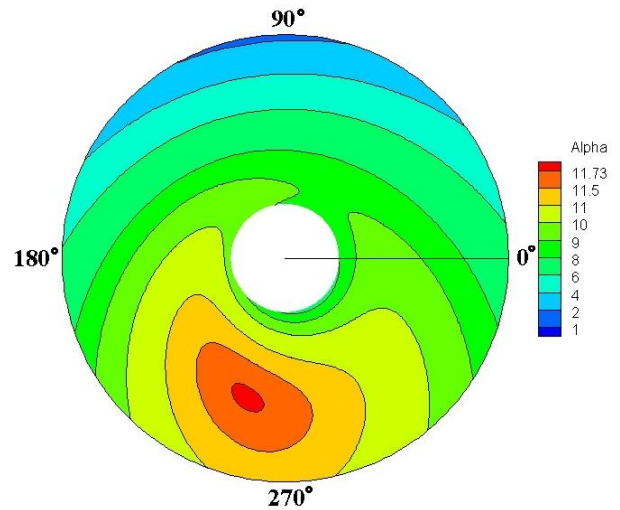$$x(t) = \frac{V_{helicopter}}{\omega} \cdot \cos(\omega t) \qquad (3)$$

Fig.2. *Distribution of angles of attack on the rotor disk*

The oscillation period corresponds to the one revolution of the rotor, but to establish a stable periodic solution 8 cycles were calculated. Each cycle was divided into 360 time steps. For each time step, 100 pseudo-time steps were performed according to the dual-time stepping method of HMB.
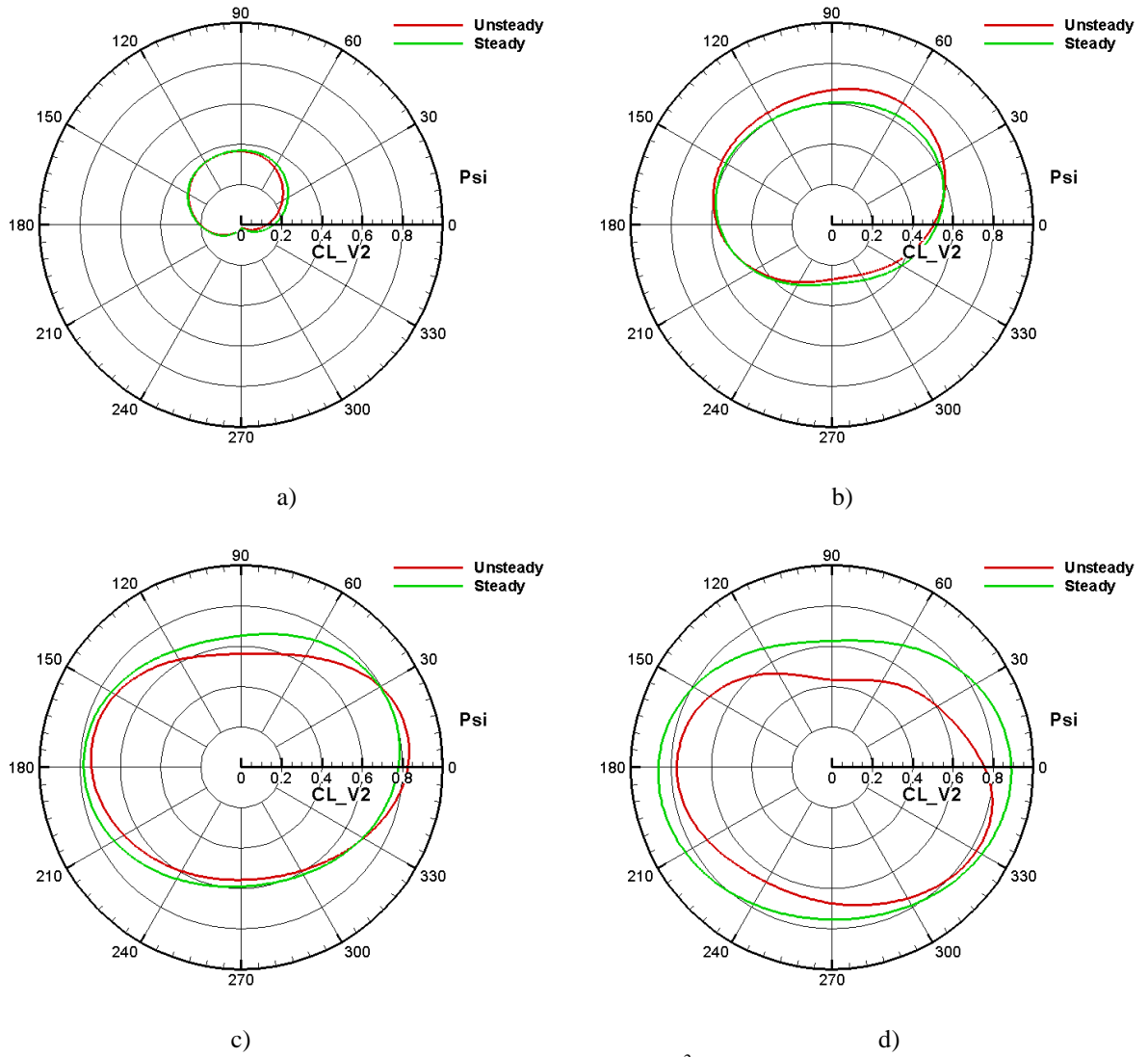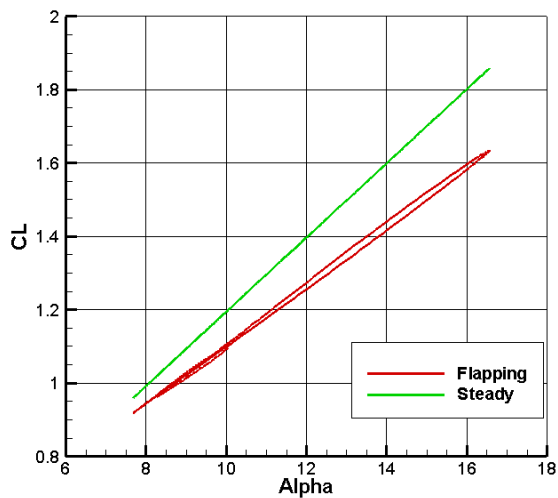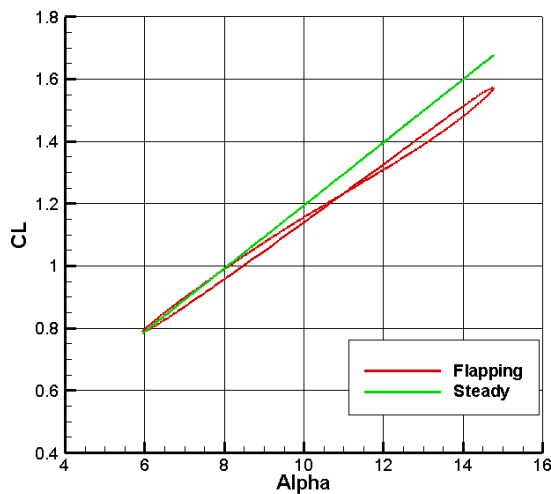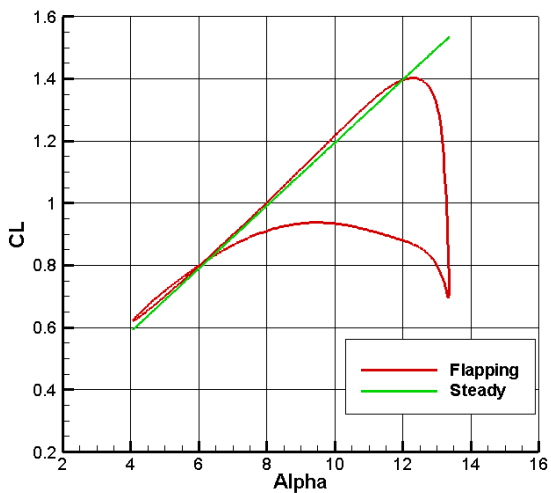
a)

b)

c)

d)

Fig.3. *Comparison of static and dynamic load* ($CL \cdot V^2$) *of the rotor blade sections:*
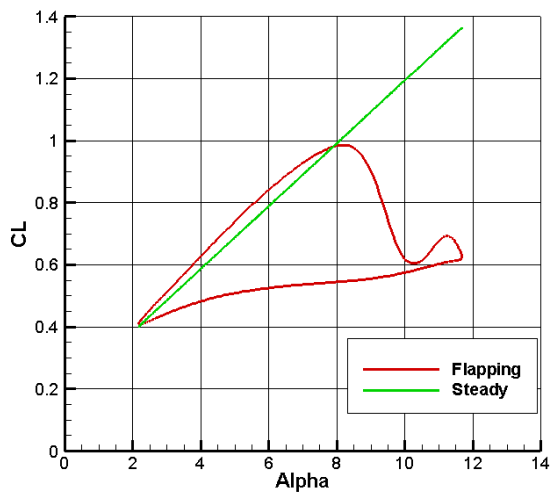*a) r=0.35; b) r=0.65; c) r=0.85; d) r=0.95*

a) b)

c) d)

Fig.4. *Steady and unsteady (flapping) lift coefficients for different sections (dimensionless radius):*
a) r=0.35; b) r=0.55; c) r=0.75; d) r=0.95

3 Results and discussion

Figure 3 shows comparisons of the results of dynamic analysis with the static characteristics of the blade sections. Static lift coefficient values are represented by linear law:

$$CL(\alpha) = A * (\alpha - \alpha_0), \qquad (4)$$

where A = 5.8 is the lift climb coefficient, α_0=-1.8° is zero lift angle of attack. Parameters (A and α_0) are correspond to experimental data [7].

As can be seen the dynamic characteristics are different from the static case, especially for the end part of advancing blade. One of the reasons for this discrepancy is that equation (4), unlike CFD, does not account for Mach number effects or stall. Compressibility of the flow, stall, impulsive effects and complex history of the shed vortices contribute to the overall hysteresis of the $CL(\alpha)$ (figure 4, 7).

To assess the impact of each component of the dynamic conditions computations were conducted for oscillating or translating cases only. The comparison of the oscillating cases with steady results is presented in figure 4.

For root part of blade, static characteristics and dynamic characteristics are close. For the end part of blade agreement is worse. The pitch oscillations lead to strong hysteresis of the lift coefficient at the tip part of blade and formula 4 is not correct for azimuth range from 180° to 360°.

It is evidently that the main reason of hysteresis is flow separation behavior. The flow during upstroke is mainly attached, then near max alpha there is a flow stall and it takes a time for the flow to re-attach during the downstroke. Figure 5 presents comparison between flow Mach number for upstroke and downstroke at the same angle of attack value. For upstroke the flow is attached but for downstroke the flow is separated.

The effect of the fore-aft aerofoil movement on the lift coefficient is presented in figure 6. The instantaneous lift coefficient values were computed using the current velocity (2). For the root part of blade the motion influences the lift

coefficients mainly at the retreating blade (ψ=180° to 360°). This influence could be significant but because of low dynamic head the loads at this part of retreating blade are not very high.

a)
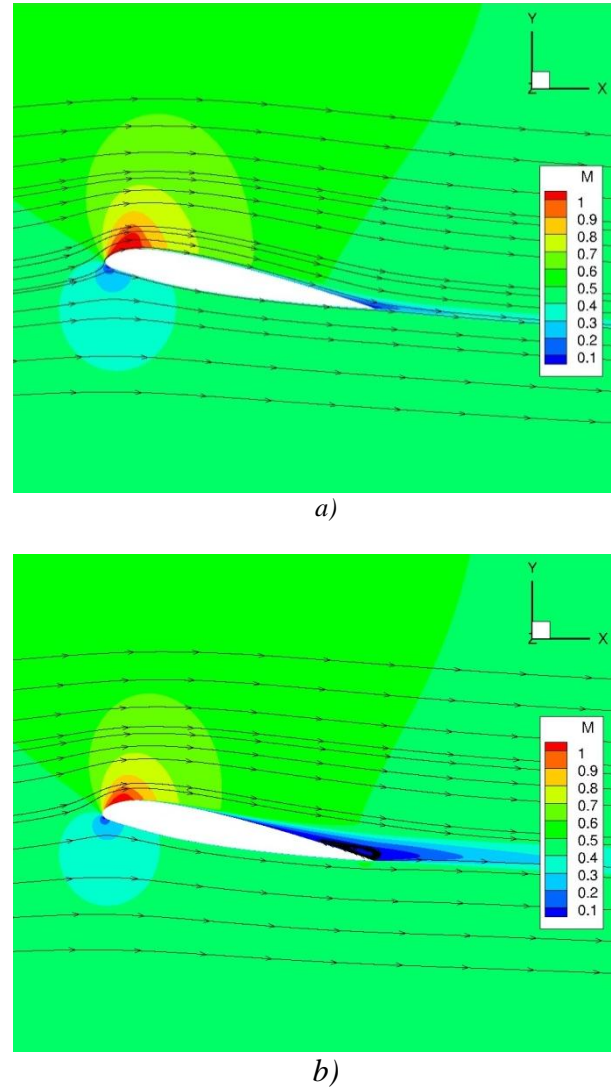

b)

Fig.5. *Comparison between (flapping) upstroke (a) and downstroke (b) at α=10˚*

For the advancing blade (ψ=0˚..180˚) the influence of the in-plane motion on the lift coefficient is stronger at the tip part of blade. The strong influence as found near ψ=90˚. A comparison of the lift coefficient behavior at different blade sections (figure 6) reveals increased lift coefficient close to the tip part of blade. This area is characterized by high values of local Mach number.
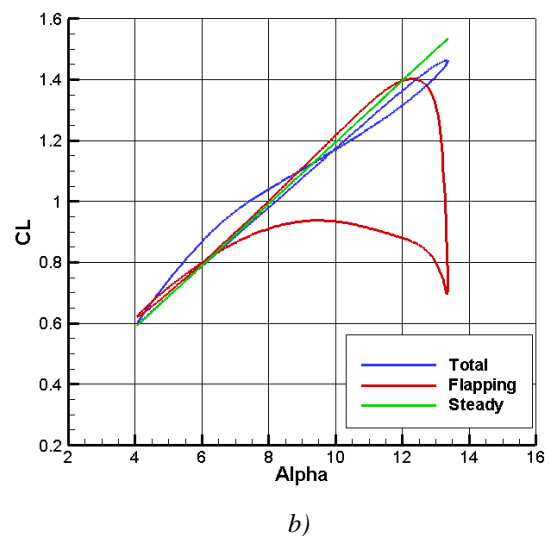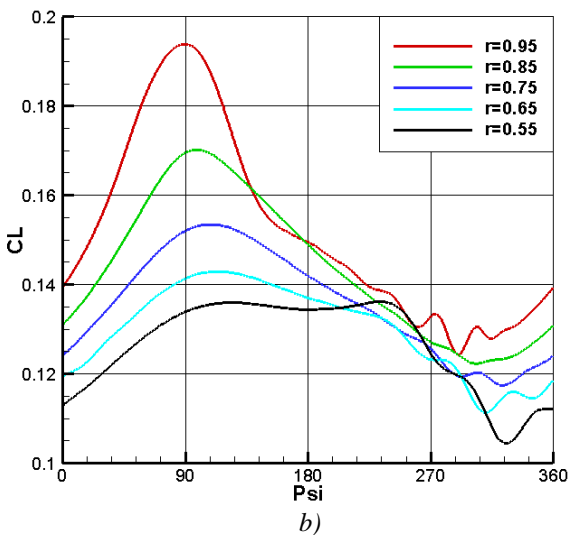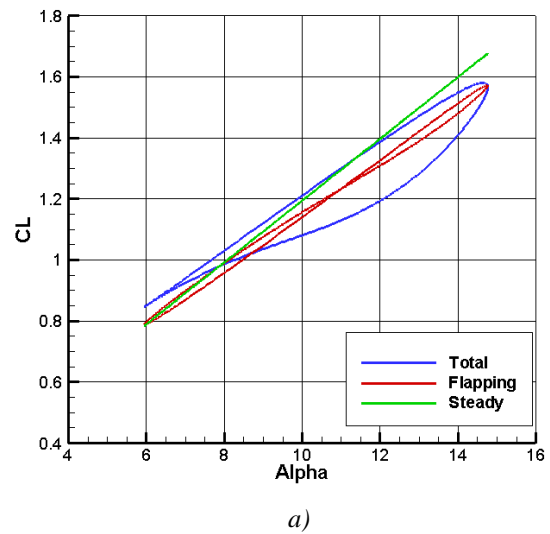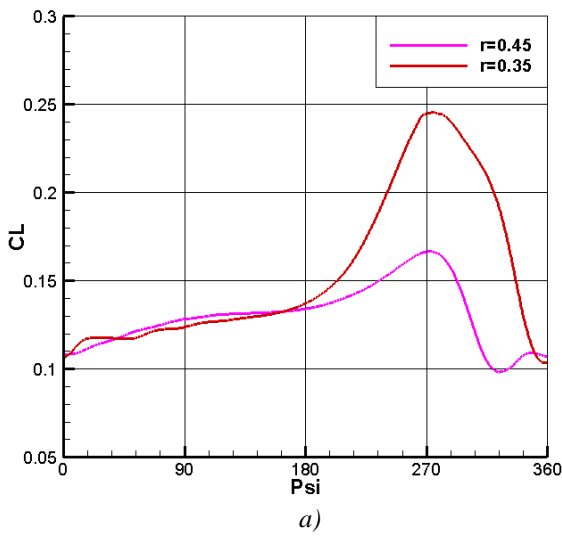
a)

b)

Fig. 6. *Influence of in-plane oscillation on the lift coefficient: a) root part of blade; b) middle and tip of blade*

a)

b)

Fig.7. *Comparison of flapping, steady and total motions with: a) r=0.55; b) r=0.75*

Figure 7 presents the lift coefficient values for different types of modeling: steady conditions, flapping motion and total motion (including pitch, and in-plane oscillations). For example, for the total motion dependence CL(α) is close to linear at *r*=0.75 section. It means that addition of reciprocating motion to flapping stabilizes flow around aerofoil with reducing of separation area (figure 8). On the contrary, at the *r*=0.55 section the flow around the aerofoil with flapping is more stable than for the total motion.
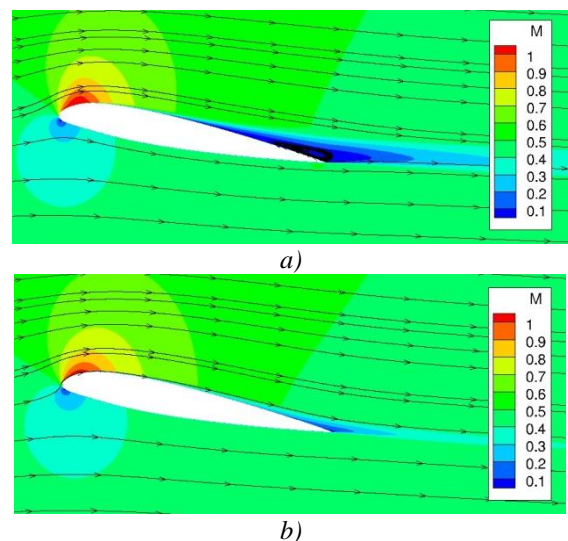

a)

b)

Fig. 8. *Comparison of flow Mach numbers around aerofoil at α=10˚ for two types of motion: flapping (a), total (b)*

4 Conclusions and Future work

Preliminary computations were presented, looking at the effect of aerofoil motion on its aerodynamic performance. For some cases, the aerodynamics performance of oscillating aerofoils can be obtained with some corrections of steady case results. For example, the in-lane oscillation can be corrected taking into account the compressibility of the flow. However, because of the complex character of the combined pitch-translation motion the resulting aerodynamics performances cannot be obtained by superposition and coupled computations with pitch and translation oscillations must be considered.

Acknowledgement

References

[1]   Barakos G. N. and Drikakis D. Computational study of unsteady turbulent flows around oscillating and ramping aerofoils. *Int. J. Numer. Meth. Fluids* 2003, 42: 163-186 pp.

[2]   Ercan Dumlupinar, V.R. Murthy. Investigation of dynamic stall of airfoils and wings by CFD. *29th AIAA Applied Aerodynamics Conference*. 27 - 30 June 2011, Honolulu, Hawaii, AIAA 2011-3511, p. 29.

[3]   Batrakov A.S., Kusyumov A.N. Investigation of flow around oscillating aerfoil. Symposium with international participation. Abstracts - "*Russian Aircraft. Problems and Prospects*". -July 2 - 5. Samara. 2012. 66 – 68 pp. [in Russian]

[4]   Menter, F. R. Two-equation eddy-viscosity turbulence models for engineering applications. *AIAA Journal,* 1994. - vol. 32, no 8. - Pp. 1598-1605.

[5]   Garipova L.I., Kusyumov A.N. Simulation of integral and distributed characteristics of the aerofoil. Flight control and navigation of aircraft. *Proceedings of the XVI All-Russian seminar on traffic management and navigation of aircraft*: Part I. Samara, 18 - 20 June 2013 - Samara, Publishing office SSC RAS, 2013, 246. - 178 - 181 pp. [in Russian]

[6]   Bramwell A. R. S., Done G. and Balmford D. *Bramwell's helicopter dynamics*. 2nd edition. Published by Butterworth-Heinemann, 2001, 372 p.

[7]   Abbott, I. H., von Doenhoff, A. E. *Theory of wing sections, including a summary of airfoil data*. Dover publication, Inc., New York, 1959.

Contact Author Email Address

Mailto: lyaysan_garipova@mail.ru

Copyright Statement